J|A|C|S
ARTICLES
Published on Web 04/15/2003

Aromatic−Aromatic Interactions in Crystal Structures of Helical Peptide Scaffolds Containing Projecting Phenylalanine Residues

Subrayashastry Aravinda,[†] Narayanaswamy Shamala,*[,†] Chittaranjan Das,[‡] Arumugam Sriranjini,[§] Isabella L. Karle,*[,||] and Padmanabhan Balaram*[,‡]

Contribution from the Department of Physics, Molecular Biophysics Unit, and Department of Inorganic and Physical Chemistry, Indian Institute of Science, Bangalore-560 012, India, and Laboratory for the Structure of Matter, Naval Research Laboratory, Washington, DC 20375-5341

Received January 11, 2003; E-mail: pb@mbu.iisc.ernet.in; shamala@physics.iisc.ernet.in

Abstract: Aromatic−aromatic interactions between phenylalanine side chains in peptides have been probed by the structure determination in crystals of three peptides: Boc-Val-Ala-Phe-Aib-Val-Ala-Phe-Aib-OMe, **I**; Boc-Val-Ala-Phe-Aib-Val-Ala-Phe-Aib-Val-Ala-Phe-Aib-OMe, **II**; Boc-Aib-Ala-Phe-Aib-Phe-Ala-Val-Aib-OMe, **III**. X-ray diffraction studies reveal that all three peptides adopt helical conformations in the solid state with the Phe side chains projecting outward. Interhelix association in the crystals is promoted by Phe−Phe interactions. A total of 15 unique aromatic pairs have been characterized in the three independent crystal structures. In peptides **I** and **II**, the aromatic side chains lie on the same face of the helix at $i/i + 4$ positions resulting in both intrahelix and interhelix aromatic interactions. In peptide **III**, the Phe side chains are placed on the opposite faces of the helix, resulting in exclusive intermolecular aromatic interactions. The distances between the centroids of aromatic pair ranges from 5.11 to 6.86 Å, while the distance of closest approach of ring carbon atoms ranges from 3.27 to 4.59 Å. Examples of T-shaped and parallel-displaced arrangements of aromatic pairs are observed, in addition to several examples of inclined arrangements. The results support the view that the interaction potential for a pair of aromatic rings is relatively broad and rugged with several minima of similar energies, separated by small activation barriers.

Introduction

Aromatic−aromatic interactions were suggested to be a stabilizing force in determining globular protein structures, from an analysis of the frequency of occurrence of aromatic pairs in protein interiors.[1−4] Burley and Petsko observed "that on an average about 60% of aromatic side chains in proteins are involved in aromatic pairs, 80% of which form networks of three or more interacting aromatic side chains. Phenyl ring centroids are separated by a preferential distance of between 4.5 and 7 Å, and dihedral angles approaching 90° are most common".[1] A large number of subsequent analyses have reemphasized the importance of aromatic interactions in structure stabilization and have pointed to the occurrence of several alternate arrangements of closely packed flat aromatic rings.[3−6] The most common idealized arrangements are schematically illustrated in Figure 1, and the parameters used to describe ring orientations are also defined.[7] Early surveys of aromatic pairs in proteins revealed a preponderance of perpendicular edge to face orientations (Figure 1d,e), although it was noted that in well-packed interiors "interaction with other side chains can interfere with and obviously overcome the preference for a perpendicular interaction in aromatic pairs".[2] A large body of experimental and theoretical work on benzene dimers[8−17] favors both the parallel-displaced (Figure 1b) and T-shaped clusters

[†] Department of Physics, Indian Institute of Science.
[‡] Molecular Biophysics Unit, Indian Institute of Science.
[§] Department of Inorganic and Physical Chemistry, Indian Institute of Science.
[||] Naval Research Laboratory.

(1) Burley, S. K.; Petsko, G. A. *Science* **1985**, *229*, 23−28.
(2) Singh, J.; Thornton, J. M. *FEBS Lett.* **1985**, *191*, 1−6.
(3) Burley, S. K.; Petsko, G. A. *J. Am. Chem. Soc.* **1986**, *108*, 7995−8001.
(4) Burley, S. K.; Petsko, G. A. *Adv. Protein Chem.* **1988**, *39*, 125−189.
(5) Hunter, C. A.; Singh, J.; Thornton, J. M. *J. Mol. Biol.* **1991**, *218*, 837−846.
(6) Serrano, L.; Bycroft, M.; Fersht, A. R. *J. Mol. Biol.* **1991**, *218*, 465−475.
(7) McGaughey, G. B.; Gagnes, M.; Rappe, A. K. *J. Biol. Chem.* **1998**, *273*, 15458−15463.
(8) Cox, E. G.; Cruickshank, D. W. J.; Smith, J. A. S. *Proc. R. Soc. London, Ser. A* **1958**, *247*, 1−21. (b) William, D. E. *Acta Crystallogr.* **1974**, *A30*, 71−74. (c) Hall, D.; Williams, D. E. *Acta Crystallogr.* **1975**, *A31*, 56−58.
(9) For examples: (a) Janda, K. C.; Hemminger, J. C.; Winn, J. S.; Novick, S. E.; Harris, S. J.; Klemperer, W. *J. Chem. Phys.* **1975**, *63*, 1419−1421. (b) Steed, J. M.; Dixon, T. A.; Klemperer, W. *J. Chem. Phys.* **1979**, *70*, 4940−4946. (c) Henson, B. F.; Hartland, G. V.; Venturo, V. A.; Felker, P. M. *J. Chem. Phys.* **1992**, *97*, 2189. (d) Ferguson, S. B.; Sanford, E. M.; Seward, E. M.; Diederich, F. *J. Am. Chem. Soc.* **1991**, *113*, 5410−5419. (e) Paliwal, S.; Geib, S.; Wilcox, C. S. *J. Am. Chem. Soc.* **1994**, *116*, 4497−4498.
(10) Hobza, P.; Selzle, H. L.; Schlag E. W. *J. Am. Chem. Soc.* **1994**, *116*, 3500−3506.
(11) Laatikainen, R.; Ratilainen, J.; Sebastian, R.; Santa, H. *J. Am. Chem. Soc.* **1995**, *117*, 11006−11010.
(12) Tsuzuki, S.; Uchimaru, T.; Mikami, M.; Tanabe, K. *Chem. Phys. Lett.* **1996**, 206−210.
(13) Jaffe, R. L.; Smith, G. D. *J. Chem. Phys.* **1996**, *105*, 2780−2788.
(14) Chipot, C.; Jaffe, R.; Maiggret, B.; Pearlman, D. A.; Kollman, P. A. *J. Am. Chem. Soc.* **1996**, *118*, 11217−11224.
(15) Hobza, P.; Selzle, H. L.; Schlag, E. W. *J. Phys. Chem.* **1996**, *100*, 18790−18794.
(16) Sun, S.; E. R. Bernstein, E. R. *J. Phys. Chem.* **1996**, *100*, 13348−13366.

10.1021/ja0341283 CCC: $25.00

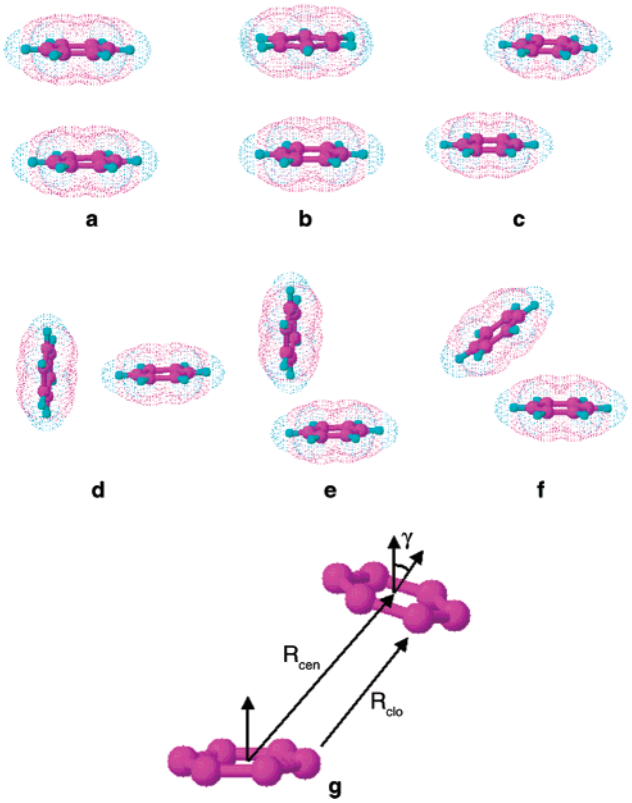

Figure 1. Geometries of aromatic interactions. The aromatic pairs are placed at a centroid−centroid distance of 5.5 Å, which is the distance at which the distribution of Phe−Phe pairs in proteins is maximum.[1] For the parallel sandwich arrangement the energetically optimum distance is expected to be at 3.5 Å. The van der Waals surfaces generated with attached hydrogen atoms are indicated: (a) parallel sandwich, eclipsed; (b) parallel sandwich, staggered; (c) parallel displaced; (d) T-shaped, edge to face; (e) L-shaped, edge to edge; (f) inclined. Parameters used to define the aromatic interaction are shown in (g): R_{cen} (Å), which is the centroid−centroid distance; γ (deg), which is the interplanar angle; R_{clo} (Å), which is the shortest distance between two carbon atoms of the interacting rings.

(Figure 1d). Indeed, while summarizing theoretical studies on benzene dimers, Sun and Bernstein note that, "if theory is telling us anything, it surely is saying that the interaction potential between two benzene molecules is quite flat and that many local minima can exist for the dimer. Only small barriers separate parallel displaced, herringbone, and perpendicular (T) conformations".[16] A more recent survey of protein structures[18] using a large dataset of 500 proteins concludes that π stacking interactions are "alive and well in proteins", a conclusion based on an analysis of isolated pairs (dimers of aromatic pairs).[7] Potential of mean force calculation lead to the conclusion that in an aqueous environment stacking is favored, whereas in hydrophobic surroundings T-shaped structures are more stable.[19] Several recent experimental studies have emphasized the importance of aromatic interactions in stabilizing helices and β-hairpins in designed synthetic peptides.[20−23] The structural properties of interacting pairs of aromatic residues have also been investigated computationally.[24] We have been investigating the effect of aromatic residue positioning on helical and β-hairpin peptide backbones. The ability to design conformationally rigid peptides of well-defined secondary structure using stereochemically constrained amino acids [25,26] has been exploited to construct helical peptides, with appropriately positioned phenylalanine (Phe) side chains. In this report, we describe the crystal structures of three helical peptides containing multiple aromatic rings, which provide an opportunity to characterize both intramolecular and intermolecular Phe−Phe interactions in the solid state. Conformational rigidity resulting in the formation of helical structure is imposed by appropriate placement of the α-aminoisobutyryl (Aib) residue.[27−30] The crystal structures of the following peptides are described:

Boc Val - Ala-**Phe-Aib-Val-Ala-Phe**- -Aib-OMe (Peptide **I**)

Boc-Val - Ala-**Phe-Aib-Val-Ala-Phe**-Aib-Val-Ala-Phe-Aib-OMe (Peptide **II**)

Boc-Aib - Ala-**Phe-Aib-*Phe*-Ala-*Val***- -Aib-OMe (Peptide **III**)

Peptides **I** and **II** contain the repeating tetrapeptide unit (Val-Ala-Phe-Aib)$_n$ (**I**, $n = 2$; **II**, $n = 3$), in which the Phe residues appear at positions i and $i + 4$ and are expected to be aligned on the same face of a helical structure. Peptide **III** contains a central Phe-Aib-Phe-Ala-Val segment, which corresponds to an interchange of the Val and Phe residues in the corresponding segment in peptide **I** and **II**, resulting in an i and $i + 2$ orientation of Phe residues, which precludes an intramolecular interaction in helical structures. Structure determination in single crystals reveals helical conformations for all three peptides and provides examples of cooperative Phe−Phe interactions throughout the crystals. Perpendicular, parallel-displaced, and inclined orientations of the interacting aromatic ring pair are observed. Peptide **II** reveals an interesting example of static disorder arising from specific Phe−Phe interaction between helical columns.

Experimental Section

Peptides **I**−**III** were synthesized by conventional solution phase procedures using a fragment condensation strategy. Boc and methyl ester groups were used as N- and C-terminal protecting groups, respectively. Peptides couplings were mediated by *N*,*N*′-dicyclohexylcarbodiimide (DCC) and 1-hydroxybenzotriazole. The peptides were purified by reverse-phase medium-pressure liquid chromatography (C_{18}, 40−60 μm) using methanol/water gradients. The peptides were characterized by 500 MHz ^{1}H NMR spectroscopy and MALDI mass

(17) Sinnokrot, M. O.; Valeev, E.; Sherrill, C. D. *J. Am. Chem. Soc*. **2002**, *124*, 10887−10893.
(18) For examples: (a) Bhattacharyya, R.; Samanta, U.; Chakrabarti, P. *Protein Eng.* **2002**, *15*, 91−100. (b) Thomas, A.; Meurisse, R.; Brasseur, R. *Proteins: Struct., Funct., Genet.*. **2002**, *48*, 635−644. (c) Thomas, A.; Meurisse, R.; Charloteaux, B.; Brasseur, R. *Proteins: Struct., Funct., Genet.* **2002**, *48*, 628−634. (d) Tóth, G.; Watts, C. R.; Murphy, R. F.; Lovas, S. *Proteins: Struct., Funct., Genet.* **2001**, *43*, 373−381. (e) Mitchell, J. B. O.; Laskowski, R. A.; Thornton, J. M. *Proteins: Struct., Funct. Genet.* **1997**, *29*, 370−380.
(19) Chelli, R.; Gervasio, F. L.; Procacci, P.; Schettino, V. *J. Am. Chem. Soc.* **2002**, *124*, 6133−6143.
(20) Butterfield, S. M.; Patel, P. R.; Waters, M. L. *J. Am. Chem. Soc*. **2002**, *124*, 9751−9755.
(21) (a) Tatko, C. D.; Waters, M. L. *J. Am. Chem. Soc*. **2002**, *124*, 9372−9373. (b) Walters, M. L. *Curr. Opin Chem. Biol.* **2002**, *6*, 736−741.
(22) Schindelin, H.; Jiang, W.; Inouye, M.; Heinemann, U. *Proc. Natl. Acad. Sci. U.S.A.* **1994**, *91*, 5119−5123.
(23) (a) Das, C.; Shankaramma, S. C.; Balaram. P. *Chem.−Eur. J.* **2001**, *7*, 840−847. (b) Aravinda, S.; Shamala, N.; Rajkishore, R.; Gopi, H. N.; Balaram, P. *Angew. Chem., Int. Ed.* **2002**, *41*, 3863−3865.
(24) Gervasio, F. L.; Chelli, R.; Procacci, P.; Schettino, V. *Proteins: Struct., Funct., Genet.* **2002**, *48*, 117−125.7
(25) Venkatraman, J.; Shankaramma, S. C.; Balaram, P. *Chem. Rev.* **2001**, *101*, 3131−3152.
(26) Kaul, R.; Balaram, P. *Bioorg. Med. Chem.* **1999**, *7*, 105−117.
(27) Prasad, B. V. V.; Balaram, P. *CRC Crit. Rev. Biochem.* **1984**, *16*, 307−347.
(28) Karle, I. L.; Balaram, P. *Biochemistry* **1990**, *29*, 6747−6756.
(29) Toniolo, C.; Benedetti, E. *Trends Biochem. Sci*. **1991**, *16*, 350−353.
(30) Balaram, P. *Curr. Opin. Struct. Biol*. **1992**, *2*, 845−851.

Table 1. Crystal and Diffraction Parameters for Peptides **I**−**III**

	peptide **I**	peptide **II**	peptide **III**
empirical formula	$C_{48}H_{72}N_8O_{11}$	$C_{69}H_{100}N_{12}O_{15}$	$2C_{47}H_{70}N_8O_{11}\cdot 4H_2O$
cryst habit	clear and rectangular	prism with cracks	clear and rectangular
cryst size (mm)	0.45 × 0.3 × 0.2	0.53 × 0.33 × 0.07	0.4 × 0.3 × 0.1
crystallizing solvent	methanol/water/acetone	acetonitrile/water	acetonitrile/water
space group	$P2_12_12_1$	$C2$	$P1$
cell params			
a (Å)	12.4460(12)	38.779(13)	10.802(3)
b (Å)	16.027(2)	8.839(2)	16.361(5)
c (Å)	27.704(3)	23.369(5)	17.853(6)
α (deg)	90.	90.	116.405(5)
β (deg)	90.	104.74(2)	95.535(7)
γ (deg)	90.	90.	93.164(6)
V (Å^3)	5526.4(11)	7746.5	2795.8(15)
Z	4	4	2
molecules/asym unit	1	1	2
cocrystallized solvent	none	none	4 water molecules
M_r	937.1	1337.6	2(923.1) + 72 = 1918.2
D_{calcd} (g/cm^3)	1.126	1.147	1.135
F(000)	2016	2872	1024
radiatn (λ, Å)	Cu Kα (1.5418)	Cu Kα (1.5418)	Mo Kα (0.710 73)
temp (°C)	21	20	21
2θ range (deg)	140.3	115.2	53.8
scan type	$\omega-2\theta$	$\theta-2\theta$	ω
scan speed	variable	constant	
indpdt reflcns	5725	5784	10 887
obsd reflcns	4140 [$\|F\| > 4\sigma(F)$]	1877 [$\|F\| > 4\sigma(F)$]	6562 [$\|F\| > 4\sigma(F)$]
final R (%)	5.88	10.22	7.68
final wR2 (%)	16.09	20.91	18.58
goodness of fit (S)	1.073	1.015	0.733
$\Delta\rho_{max}$ (e Å^{-3})	0.64	0.24	0.45
$\Delta\rho_{min}$ (e Å^{-3})	−0.20	−0.24	−0.23
no.of restraints/params	6/605	14/768	5/1225
data-to-param ratio	6.8:1	2.45:1	5.4:1

spectrometry (M_{Na^+} = 959.8, M_{cal} = 937.1 for peptide **I**; M_{Na^+} = 1360.5, M_{cal} = 1337.6 for peptide **II**; M_{Na^+} = 945.4, M_{cal} = 923.1 for peptide **III**).

Crystals of peptide **I** were grown from methanol/water mixtures by slow evaporation. Three-dimensional intensity data were collected up to 140° using Cu Kα radiation (λ = 1.5418 Å) on a CAD4 diffractometer. The structure was determined and refined (SHELXS-97 and SHELXL-97)[31] to an R factor of 5.88%.

Crystals of peptide **II** grown from dioxane/methanol were very thin and fragile. Robust prisms were obtained by slow evaporation from acetonitrile/water solution. Even though most of the crystals contained cracks, the optical extinction was good and the X-ray peaks generally had a good profile. X-ray data were collected for a triclinic setting with Cu Kα radiation (λ = 1.5418 Å). The structure was solved initially in space group $P1$ for the two molecules in the unit cell, using a vector search procedure[32,33] and tangent formula expansion[34] based on a 34 atom model from the α-helical structure of Ac-Val-Ala-Leu-Dpg-Val-Ala-Leu-OMe.[35] The two molecules in the cell were very similar, including the disorder in the three phenylalanine residues. Furthermore, they were related by a rotation axis. The X-ray data were recollected in the more symmetric monoclinic space group $C2$, in which there is one molecule/asymmetric unit. In both space groups, at the Phe(3), Phe(5), and Phe(11) residues, there are two positions for each phenyl ring, with about 50% occupancy in each position. Because of the proximity of many atoms of the phenyl rings in the "average" electron density map, the six phenyl rings were restrained to have idealized values for C−C = 1.39 Å and C−C−C = 2.41 Å and refined isotropically. Additionally, there are two positions for the *tert*-butyl group in the terminal *tert*-butoxy group related by a rotation about a C−O bond. Full-matrix least-squares refinement resulted in an R factor of 10.2%.

Crystals of peptide **III** were grown by slow evaporation of acetonitrile/water mixture in the triclinic space group $P1$, with two molecules in the asymmetric unit, along with four water molecules. The X-ray data were collected on a Bruker AXS SMART APEX CCD diffractometer, using Mo Kα radiation (λ = 0.710 73 Å). The structure was solved by direct methods[36] and refined to an R factor of 7.68%. The crystal and diffraction parameters for peptides **I**−**III** are summarized in Table 1.

Results and Discussion

Figure 2 shows a view of the molecular conformation of the three peptides determined in crystals. The backbone and side chain torsion angles are summarized in Table 2, and hydrogen bond parameters are listed in Table 3. Peptides **I** and **II** exhibit predominantly a pattern of a α-helical (5→1 hydrogen bonds) with good 4→1 hydrogen bonds (3_{10}-helical turns) observed only at the termini. The observed hydrogen bonds listed in Table 3 are based on a comparison of all the parameters for both 4→1 and 5→1 interactions.[37,38]

The structure of an "averaged" molecule of peptide **II** with 2-fold disorder is shown in Figure 2b. All the valine side chains are on one side of the helix, and all the disordered phenylalanine

(31) (a) Sheldrick, G. M. *SHELXS 97, Program for Automatic Solution of Crystal Structures*; University of Göttingen: Göttingen, Germany, 1997. (b) Sheldrick, G. M. *SHELXL 97, Program for crystal structure refinement*; University of Göttingen: Göttingen, Germany, 1997.
(32) Nordman, C. E.; Nakatsu, K. *J. Am. Chem. Soc*. **1963**, *85*, 353−354.
(33) Egert, E.; Sheldrick, G. M. *Acta Crystallogr*. **1985**, *A41*, 262−268.
(34) Karle, J. *Acta Crystallogr*. **1968**, *B24*, 182−186.
(35) Vijayalakshmi, S.; Rao, R. B.; Karle, I. L.; Balaram, P. *Biopolymers* **2000**, *53*, 84−98.
(36) Sheldrick, G. M.; Schneider, T. R. *Direct Methods for Macromolecules. Methods in Macromolecular Crystallography*; Turk, D., Johnson, L., Eds.; IOS Press: Amsterdam, 2001; pp 72−81.
(37) Datta, S.; Shamala, N.; Banerjee, A.; Balaram, P. *J. Pept. Res.* **1997**, *49*, 604−611.
(38) Baker, E. N.; Hubbard, R. E. *Prog. Biophys. Mol. Biol*. **1984**, *44*, 97−179.

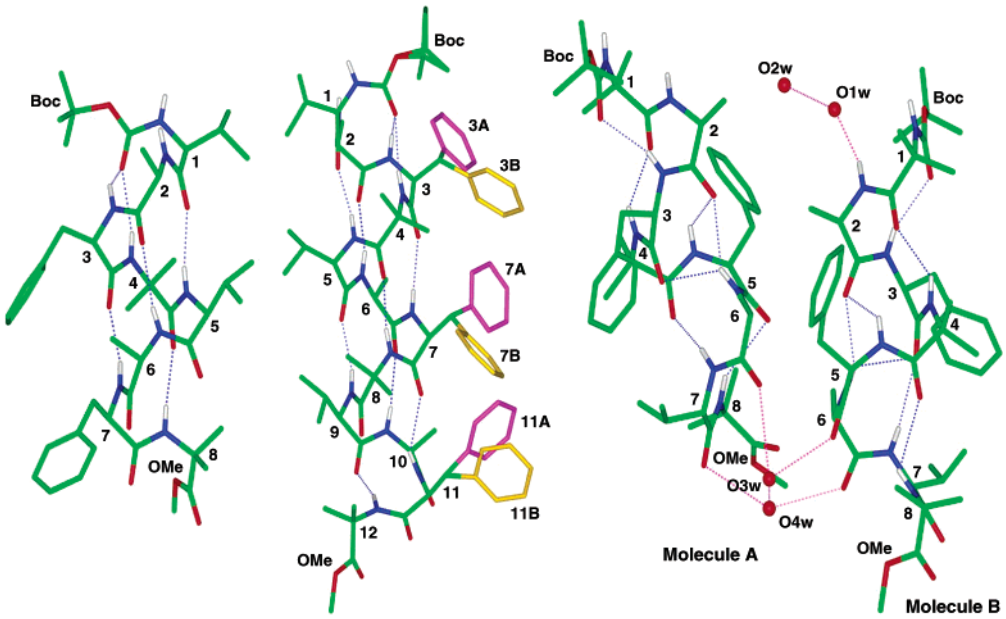

Figure 2. Molecular conformation in crystals of peptides **I**−**III**. All the hydrogen bonds are shown as dotted lines: (a) **I**, Boc-Val-Ala-Phe-Aib-Val-Ala-Phe-Aib-OMe; (b) **II**, Boc-Val-Ala-Phe-Aib-Val-Ala-Phe-Aib-Val-Ala-Phe-Aib-OMe; (c) **III**, Boc-Aib-Ala-Phe-Aib-Phe-Ala-Val-Aib-OMe.

Table 2. Torsion Angles (deg)[45] for Peptides **I**−**III**

	ϕ				Ψ				ω			
residue	I	II	IIIA	IIIB	I	II	IIIA	IIIB	I	II	IIIA	IIIB
Val(1)/Aib(1)	−55.8[a]	−50.5[a]	−53.2[a]	−55.7[a]	−37.6	−42.2	−35.8	−31.9	−179.7	−176.8	−176.6	−179.8
Ala(2)	−56.4	−58.5	−57.0	−53.7	−38.4	−40.8	−28.8	−30.8	176.0	−177.6	−178.6	−179.5
Phe(3)	−69.7	−69.5	−61.8	−60.2	−45.0	−47.1	−38.0	−37.5	179.3	180	179.8	177.0
Aib(4)	−51.3	−52.2	−53.7	−54.2	−46.9	−47.1	−44.4	−46.0	−177.6	−178.8	−178.8	−179.1
Val(5)/Phe(5)	−63.3	−63.1	−68.3	−66.6	−44.9	−45.0	−30.9	−39.6	−179.7	178.2	−179.6	−172.8
Ala(6)	−64.5	−54.5	−63.9	−68.7	−39.2	−45.7	−21.5	−32.7	−179.6	171.2	−179.9	179.7
Phe(7)/Val(7)	−64.5	−54.3	−109.8	−104.3	−44.3	−50.2	−7.8	−3.1	170.5	−179.9	−172.6	−175.6
Aib(8)	51.0	−59.8	−66.9	−54.0	49.1[b]	−37.2	161.1[b]	−35.1[b]	171.3[c]	177.6	168.6[c]	−178.3[c]
Val(9)		−63.1				−47.6				−175.3		
Ala(10)		−60.9				−28.9				−175.1		
Phe(11)		−103.8				−9.1				−161.9		
Aib(12)		−68.5				165.5[d]				173.8[e]		

Side Chain Torsion Angles (deg)

	$\chi1$				$\chi2$			
residue	I	II	IIIA	IIIB	I	II	IIIA	IIIB
Val(1)	−61.1, 174.2	−33.7, −147.0						
Phe(3)	172.6	−78.6 (178.7)	−171.7	−170.1	70.9, −108.2	83.6, −100.9 (58.8, −117.7)	78.8, −96.7	66.8, −112.2
Val(5)/Phe(5)	−72.6, 163.7	−70, 166.2	−69.6	−65.5			87.2, −99.9	86.9, −93.6
Phe(7)/Val(7)	−174.1	−73.7 (167.4)	75.4, −55.1	66.1, −55.3	78.6, −100.8	107.6, −69.6 (74.7, −101.6)		
Val(9)		−65.5, 167.3						
Phe(11)		−49.0 (−90.9)				153.0, −34.2 (91.6, −96.5)		

[a] C′(0)−N(1)−C$^{\alpha}$(1)−C′(1). [b] N(8)−C$^{\alpha}$(8)−C′(8)−O(OMe). [c] C$^{\alpha}$(8)−C′(8)−O(OMe)−C(OMe). [d] N(12)−C$^{\alpha}$(12)−C′(12)−O(OMe). [e] C$^{\alpha}$(12)−C′(12)−O(OMe)−C(OMe). The side chain torsion angle values of disordered Phe residues in peptide **II** are given in parentheses. Esd's ≈ 1.0°

side chains are on the other side. The "averaged" molecule represents two distinct conformers where rotations take place about the C$^{\alpha}$−C$^{\beta}$ bonds. In conformer A, where the three phenyl rings point upward, the torsion angles N$_i$C$^{\alpha}{}_i$C$^{\beta}{}_i$C$^{\gamma}{}_i$ ($\chi^1{}_i$) are −79, −74, and −49° (*gauche*$^-$, *g*$^-$) for rings labeled 3A, 7A, and 11A. In conformer B, where the rings point downward, the torsion angles are 179, 167, and −91° (*trans*, *t*) for rings labeled 3B, 7B, and 11B. The *g*$^+$ and *t* side chain conformation have a greater propensity for occurrence for Phe residues in α-helices in proteins.[39]

(39) Chakrabarti, P.; Pal, D. *Prog. Biophys. Mol. Biol.* **2001**, *76*, 1−102.

Peptide **III** crystallized with two molecules in the asymmetric unit. Molecule A showed a predominately 3_{10}-helical (4→1 hydrogen-bonding pattern), while molecule B revealed a mixed 3_{10}/α helix, with the N and C terminal segment stabilized by 4→1 and 5→1 hydrogen bonds, respectively. A comparison of N···O and H···O distances listed in Table 3 suggests that the intramolecular hydrogen bonds in peptide **III** are significantly weaker on an average than those observed in peptides **I** and **II**. This observation may be of some significance in the light of the subsequent discussion of the array of aromatic−aromatic interactions that stabilize the molecules in the crystal. It is

Table 3. Hydrogen Bonds for Peptides **I**−**III**

type	donor	acceptor	N···O (Å)	H···O (Å)	C═O···H (deg)	C═O···N (deg)	O···HN (deg)
		Peptide **I**: Intermolecular Bonds					
	N(1)	O(6)[a]	3.088	2.232	158.6	157.5	173.8
	N(2)	O(7)[a]	2.872	2.040	155.3	153.4	162.4
		Peptide **I**: Intramolecular Bonds					
4→1	N(3)	O(0)	2.993	2.397	114.5	125.4	126.8
5→1	N(4)	O(0)	3.177	2.331	155.2	158.4	167.6
5→1	N(5)	O(1)	2.959	2.114	161.9	164.5	167.2
5→1	N(6)	O(2)	3.193	2.383	137.5	142.8	157.3
5→1	N(7)	O(3)	2.931	2.092	161.3	164.6	165.2
5→1	N(8)	O(4)	3.058	2.204	151.1	153.2	172.3
		Peptide **II**: Intermolecular Bonds					
	N(1)	O(10)[b]	2.924	2.244	142.3	155.0	132.0
	N(2)	O(11)[c]	2.905	2.070	148.1	146.9	153.8
		Peptide **II**: Intramolecular Bonds					
4→1	N(3)	O(0)	2.985	2.367	118.4	129.4	125.9
5→1	N(4)	O(0)	3.195	2.307	155.6	158.6	168.9
5→1	N(5)	O(1)	2.907	2.030	161.0	164.1	164.5
5→1	N(6)	O(2)	3.090	2.254	134.1	141.1	154.4
5→1	N(7)	O(3)	3.069	2.178	158.0	158.8	170.3
5→1	N(8)	O(4)	3.064	2.184	151.7	155.4	165.6
5→1	N(9)	O(5)	2.963	2.103	155.5	159.7	159.7
5→1	N(10)	O(6)	3.105	2.251	144.7	149.5	158.4
5→1	N(11)	O(7)	3.154	2.397	149.9	159.6	141.8
4→1	N(12)	O(9)	3.365	2.484	102.1	105.4	166.3
		Peptide **III**, Molecule **A**: Intermolecular Bonds					
	N(1)[d]	O(7)	2.983	2.142	153.1	155.0	166.0
	N(2)[d]	O4w	2.911	2.082			161.6
		Peptide **III**, Molecule **A**: Intramolecular Bonds					
4→1	N(3)	O(0)	2.976	2.172	125.0	129.7	155.7
4→1	N(4)	O(1)	3.064	2.408	118.7	127.8	133.5
4→1	N(5)	O(2)	3.165	2.635	99.6	111.8	121.1
4→1	N(6)	O(3)	2.994	2.404	97.4	110.4	126.3
5→1	N(6)	O(2)	3.183	2.451	145.3	154.4	143.3
4→1	N(7)	O(4)	3.382	2.593	106.4	112.7	153.1
4→1	N(8)	O(5)	3.295	2.511	96.4	103.5	151.9
solvent	O3w	O(6)	3.188				
solvent	O4w	O(7)	3.248				
solvent	O3w	O4w	2.711				
		Peptide **III**, Molecule **B**: Intermolecular Bonds					
	O1w[d]	O(7)	2.757				
		Peptide **III**, Molecule **B**: Intramolecular Bonds					
4→1	N(3)	O(0)	3.026	2.212	128.2	132.4	157.9
4→1	N(4)	O(1)	3.061	2.401	118.6	127.5	134.0
4→1	N(5)	O(2)	3.149	2.622	102.1	114.2	120.6
4→1	N(6)	O(3)	3.080	2.528	96.5	109.5	122.8
5→1	N(6)	O(2)	3.119	2.358	148.2	156.6	147.6
5→1	N(7)	O(3)	3.229	2.436	158.1	161.7	153.5
5→1	N(8)	O(4)	3.166	2.642	138.1	149.3	120.4
solvent	N(2)	O1w	2.932	2.099			162.9
solvent	O1w	O2w	3.476				
solvent	O3w	O(5)	2.877				
solvent	O4w	O(6)	2.931				

[a] Symmetrically related by $-x + 1/2 + 1, -y, z + 1/2$. [b] Symmetrically related by $x + 1/2, y + 1/2, z$. [c] Symmetrically related by $x + 1/2, y - 1/2, z$. [d] Symmetrically related by $x, y + 1, z$.

conceivable that optimization of intermolecular interactions may compensate for weaker intrachain hydrogen bonds.

Helix Packing. In crystals of peptide **I** adjacent helical columns are packed in antiparallel fashion along the crystallographic *b*-axis (Figure 3a). Along the *a*-axis helical columns are arranged in parallel rows resulting in a pseudo hexagonal grid arrangement.[40] A similar packing mode of the approximately cylindrical helical structure is observed in crystals of **II** (Figure 3b). No solvent molecules were observed in crystals of peptides **I** and **II**, with vertical columns of helices formed exclusively by head-to-tail hydrogen bonds, between the free NH and CO groups at helix termini. In peptide **III**, the asymmetric unit consists of a pair of approximately parallel helices. The helical columns are arranged in, necessarily, parallel fashion in the triclinic crystal (Figure 4a). As many as four water molecules are located in the head-to-tail region providing hydrogen bonds, which hold helical columns together and also facilitate the interaction of adjacent columns (Figure 4b).

Figures 5 −7 provide a schematic view of the three helical peptide molecules, illustrating the interaction between the Phe side chains. The centroid−centroid distances are marked. In peptides **I** and **II** the interactions are both intra- and interhelical. In peptide **III** an array of intermolecular Phe−Phe contacts bridges helical peptides in the crystals. As noted earlier in peptide **II** the Phe side chains adopts two different conformations (conformers A and B) as shown in Figure 6a. They are distinct from each other. The phenyl rings must all point in the same direction for spatial considerations, that is, to avoid collisions with each other. The directions in which the Phe rings point appear to be equally acceptable.

Aromatic−Aromatic Interactions. Figure 8 summarizes the relative orientation of the 15 unique aromatic pairs structurally characterized in peptides **I**−**III**. Three parameters have been used to describe the aromatic pair geometries: R_{cen} (Å), which is the centroid−centroid distance. γ (deg), which is the interplanar angle, and R_{clo} (Å), which is the shortest distance between two carbon atoms. It is evident from the Figure 8 that two examples in peptide **I** Phe(3)(x, y, z)−Phe(7)($-x + 1, y - 1/2, -z - 1/2$) and Phe(7)($x, y, z$)−Phe(3)($-x + 1, y + 1/2, -z - 1/2$) (Figure 8b,c) correspond to parallel-displaced conformations with a very low value of γ. Four examples, Phe(11B)($1/2 - x, y - 1/2, 2 - z$)−Phe(3A)(x, y, z) and Phe(11A)-($1/2 - x, y - 1/2, 2 - z$)−Phe(3B)(x, y, z) in peptide **II** (Figure 8e,k) and Phe(3)B(x, y, z)−Phe(5)B($x + 1, y, z$) and Phe(5)A-(x, y, z)−Phe(3)A($x + 1, y, z$) in peptide **III** (Figure 8 l,n) are close to the T-structure in which the benzene rings are approximately perpendicular and arranged in an edge-to-face manner, with γ greater than 75°. Of the remaining nine examples, two have relatively large γ values (>60°) Phe(5)B($x + 1, y, z$)−Phe(5)A(x, y, z) and Phe(3)A($x + 1, y, z$)−Phe-(5)B($x, y, z - 1$) in peptide **III** (Figure 8m,o) and could be broadly classified under the T category. The remaining seven examples Phe(3)(x, y, z)−Phe(7)(x, y, z) in peptide **I** (Figure 8a) and Phe(11B)($1/2 - x, y - 1/2, 2 - z$)−Phe(7B)($1/2 - x, y - 1/2, 2 - z$), Phe(3A)(x, y, z)−Phe(7B)($1/2 - x, y - 1/2, 2 - z$), Phe(7A)(x, y, z)−Phe(3B)($1/2 - x, y - 1/2, 2 - z$), Phe-(3A)(x, y, z)−Phe(7A)(x, y, z), Phe(7A)(x, y, z)−Phe(11A)(x, y, z), and Phe(11A)(x, y, z)−Phe(3B)($-x, y, 2 - z$) in peptide **II** (Figure 8d,f−j) have γ values between 25 and 50°, corresponding to inclined arrangements. It may be noted that the R_{clo} value of 2.31 Å obtained for 7A−3B interaction in peptide **II** is unacceptably close. The temperature factors for C7D, C7E, and C7Z (conformer A) are high indicating substantial uncertainty in the crystallographically determined positions. It should be noted that a small rotation (≈30°) about the axis through the 1 and 4 positions of the benzene ring 7A relieves the close 7A−3B approach without changing the centroid−centroid

(40) (a) Karle, I. L. *Acta Crystallogr.* **1992**, *B48*, 341−356. (b) Karle, I. L. *Biopolymers* **1996**, *40*, 157−180. (c) Karle, I. L. *Acc. Chem. Res.* **1999**, *32*, 693−701.

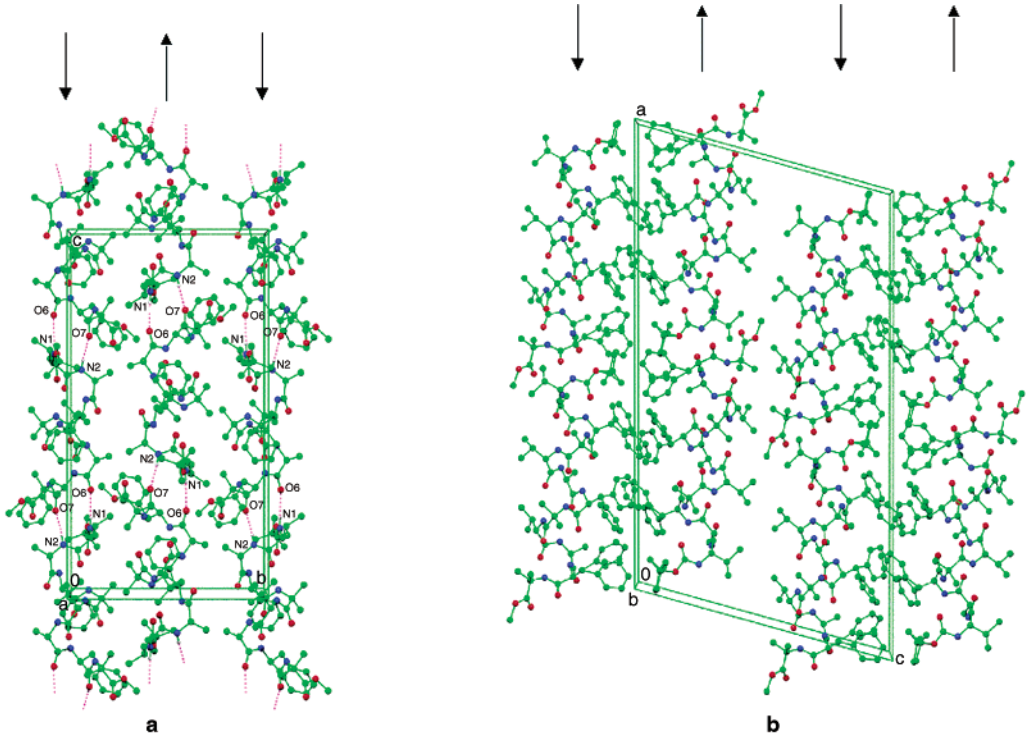

Figure 3. Molecular packing of peptide **I** and **II** in crystals: (a) **I**, Boc-Val-Ala-Phe-Aib-Val-Ala-Phe-Aib-OMe; (b) **II**, Boc-Val-Ala-Phe-Aib-Val-Ala-Phe-Aib-Val-Ala-Phe-Aib-OMe. The arrows indicate the direction of the helix axes.

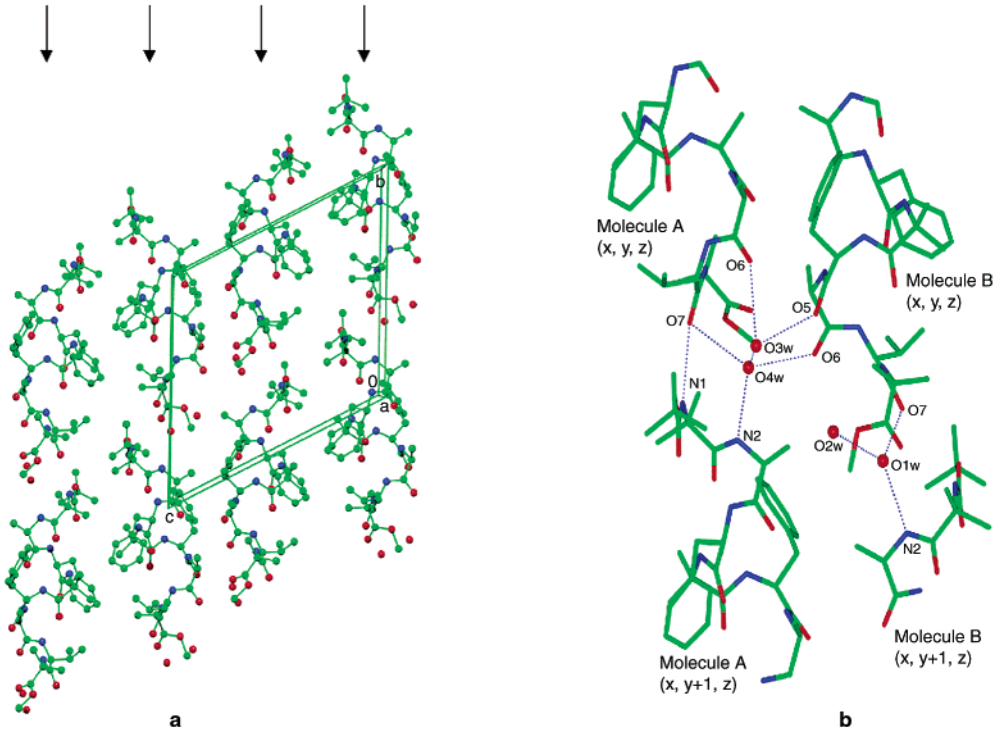

Figure 4. (a) Molecular packing of **III**, Boc-Aib-Ala-Phe-Aib-Phe-Ala-Val-Aib-OMe, in crystals. Arrows indicate the direction of the helix axes. (b) Environment of the water molecules which hold helical columns together and provide stabilizing intracolumn and intercolumn interactions.

distance. To further increase the R_{clo} distance between 7A and 3B, a similar rotation can also take place in ring 3B.

The results suggest that there is no dominant preference for a specific geometrical arrangement of the proximal aromatic rings in these structures. However, some of the observed arrangements correspond closely to the T-shaped and parallel-displaced structures commonly observed in proteins and postulated as energy minima in theoretical calculations. The arrangement of two proximal aromatic rings is expected to be dominated by quadrupole−quadrupole interactions, which are anticipated to have a strong angular dependence.[4,41] The interesting observation that quadrupole−quadrupole interactions may be destabilizing in a face to face geometry has been emphasized.[42] The present observations reinforce a view that

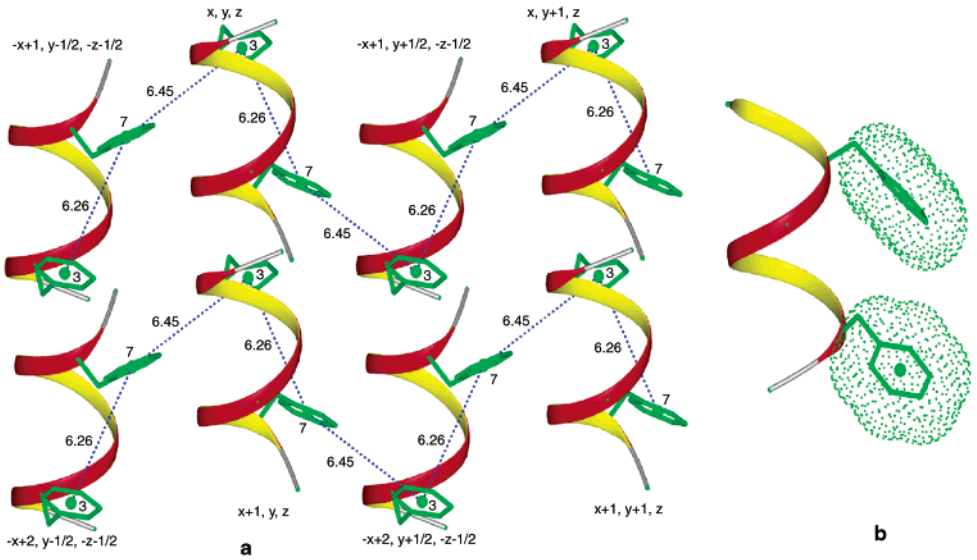

Figure 5. (a) Schematic view of the Phe−Phe interactions in crystals of peptide **I**. The molecular backbone is shown as a ribbon representation, and the centroid to centroid distances (Å) between proximal aromatic rings are marked. (b) Schematic view of a proximal Phe−Phe interaction on the surface of the helix in peptide **I**. The residues shown are Phe(3) and Phe(7). The representation was generated using the program MOLMOL.[46]

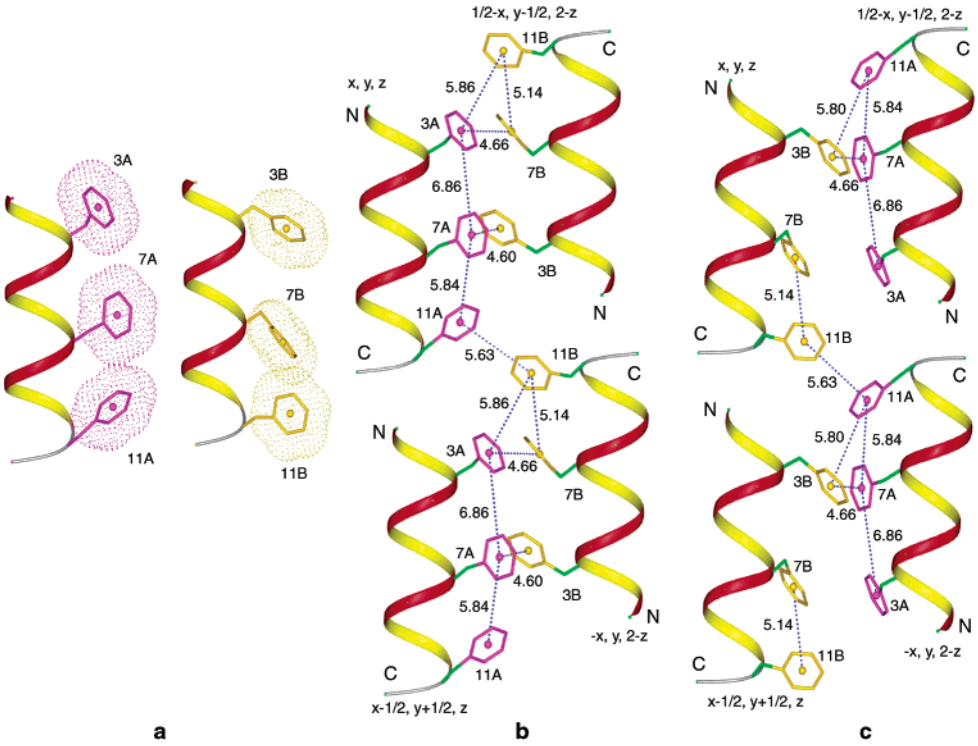

Figure 6. Schematic view of the Phe−Phe interactions in crystals of peptide **II**: (a) two sets of Phe conformations separately indicated on a helical scaffold; (b, c) two alternate sets of Phe−Phe interactions observed between helical molecules which form antiparallel columns in the crystals. The centroid to centroid distances (Å) are indicated.

is emerging from computational studies of benzene dimers that the potential energy surface for an interacting pair of aromatic ring is relatively flat with local minima which are separated by very small energy barriers.[16]

A particular interesting consequence of the aromatic interactions on crystal packing is observed in the structure of peptide **II**. The three aromatic rings of the Phe side chains at positions 3, 7, and 11 are aligned on the same face of the helix. Opposing antiparallel column of helices interact through the projecting aromatic side chains as schematically illustrated in Figure 6b,c. An interacting ladder of phenylalanine side chains is present with opposing pairs forming rungs of the ladder. Close approaches of aromatic rings on the same molecule corresponding to a stabilizing interaction between the rungs of the ladder are also observed. Crystallographically, the three Phe side chains occupy two distinct spatial positions, characterized by distinct

(41) (a) Brown, N. M. D.; Swinton, F. L. *J. Chem. Soc., Chem. Commun*. **1974**, 770. (b) Hunter, C. A.; Sanders, J. K. M. *J. Am. Chem. Soc.* **1990**, *112*, 5525−5534. (c) Hunter, C. A.; Lawson, K. R.; Perkins, J.; Urch, C. J. *J. Chem. Soc., Perkin Trans. 2* **2001**, 651−669.

(42) Shetty, A. S.; Zhang, J.; Moore, J. S. *J. Am. Chem. Soc*. **1996**, *118*, 1019−1027.

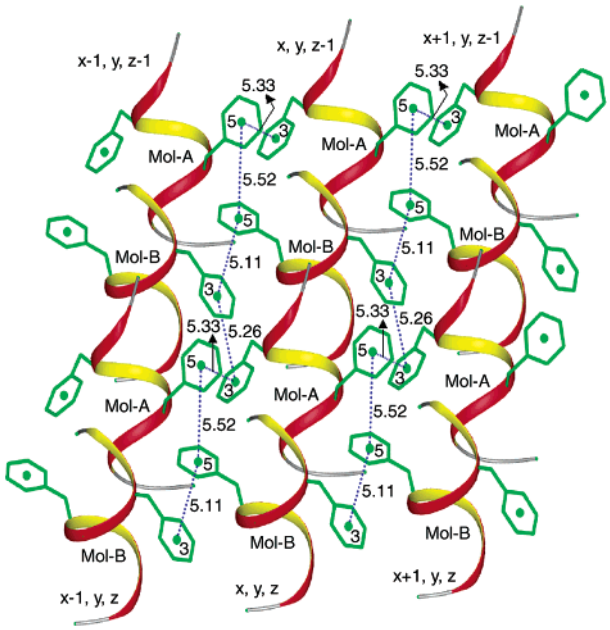

Figure 7. Schematic view of the Phe−Phe interactions observed in crystals of peptide **III**. The centroid to centroid distances (Å) are indicated. Note that there are no intramolecular Phe−Phe interactions in this peptide.

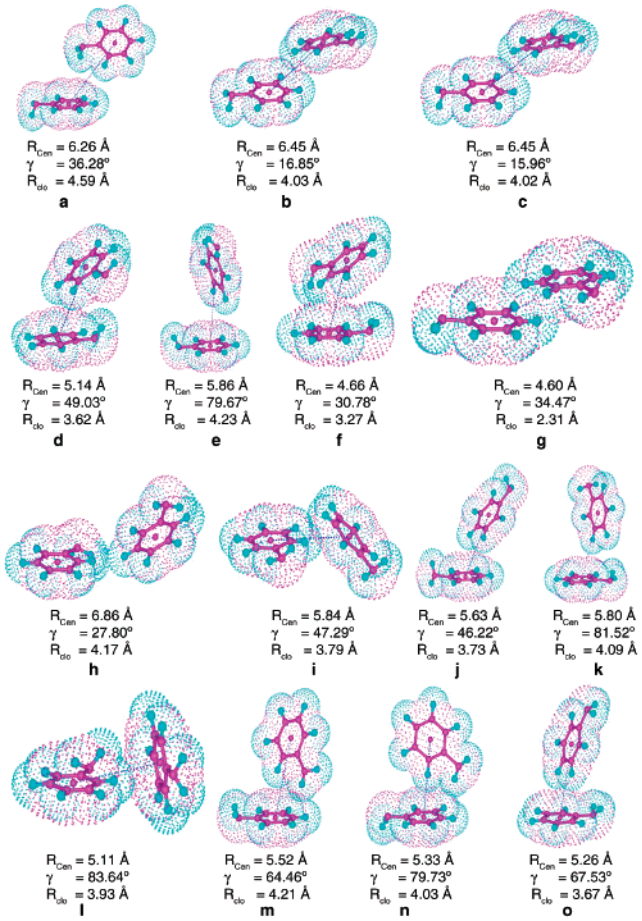

Figure 8. Summary of the unique aromatic−aromatic interactions observed in the crystals of peptides **I**−**III**. The parameters R_{cen}, γ, and R_{clo} are indicated: (a−c) peptide **I**; (d−k) peptide **II**; (l−o) peptide **III**. The interacting Phe side chains are shown as benzyl groups with attached hydrogens. The van der Waals surfaces are shown.

Phe side chain conformations. Particularly noteworthy is the fact that in opposing columns of helices if the Phe side chain at positions 3, 7, and 11 adopts conformation A, then the facing set of Phe residues adopts conformation B, a clear indication that specific arrangements of aromatic rings stabilize interhelix packing. There is, however, no long-range correlation between the ring conformations in the crystal resulting in a statistical distribution of helical column pairs, such that on an average half the molecules adopt conformation A, while the other half adopts conformation B, resulting in an occupancy factor of 0.5 for the individual conformations. Interestingly, the isopropyl side chains of Val residues, which occur on the other face of the helical molecules, are not disordered in the crystals.

Conclusions

This study illustrates the use of helical peptide scaffolds for probing the nature of aromatic side chain interactions in designed peptides, where the spatial disposition of the side chains can be controlled by placing aromatic residues at appropriate sequence positions. The crystallinity of hydrophobic helical peptides containing Aib residues, which act as stereochemical directors of peptide chain folding, permits precise structural characterization of these interactions by X-ray diffraction. The analysis of 15 unique aromatic pairs in three independent helical peptide crystal structures provides examples of T-shaped, parallel-displaced, and inclined arrangement of interacting Phe rings. The experimental observations are generally consistent with the view that the energy landscape for a pair of interacting phenyl rings consists of a broad, relatively flat minimum, which appears to be some what rugged, with several local minima separated by small energy barriers. In crystals, cooperative interactions between aromatic rings can lead to interesting examples of disorder in the solid state, as exemplified by the structure of the dodecapeptide **II** containing three Phe residues. Cooperative aromatic interactions may prove to be an important determinant of biological structures and have been recently suggested to be important in self-assembly of amyloid fibrils.[43] An interesting recent crystal structure of the tetrapeptide Phe-Gly-Phe-Gly reveals a fully extended, flat, sheet conformation.[44] The absence of buckling or pleating of the peptide chain may have its origin in the observed network of aromatic interaction in the crystals.

Acknowledgment. This work was supported by a program grant in the area of Drug and Molecular Design by the Department of Biotechnology, a grant from the Council of Scientific and Industrial Research of India. The CCD diffractometer facility was supported by the IRPHA program of the Department of Science and Technology of India. The work at Naval Research Laboratory was supported by the National Institutes of Health, Grant GM-30902, and the Office of Naval Research.

Supporting Information Available: X-ray crystallographic files for peptide **I**−**III** (CIF format). This material is available free of charge via the Internet at http://pubs.acs.org.

JA0341283

(43) (a) Gazit, E. *FASEB J.* **2002**, *16*, 77−83. (b) Gazit, E. *Curr. Med. Chem.* **2002**, *9*, 1667−1675.
(44) Birkedal, H.; Schwarzenbach, D.; Pattison, P. *Chem. Commun.* **2002**, 2812−2813.
(45) IUPAC−IUB Commission on Biochemical Nomenclature. *Biochemistry* **1970**, *9*, 3471−3479.
(46) Koradi, R.; Billeter, M.; Wuthrich, K. *J. Mol. Graphics* **1996**, *14*, 51−55.